Springer

KSME

Journal of Mechanical Science and Technology 27 (8) (2013) 2547~2555
www.springerlink.com/content/1738-494x
DOI 10.1007/s12206-013-0639-0

Influence of steam injection and hot gas bypass on the performance and operation of a combined heat and power system using a recuperative cycle gas turbine †

Soo Young Kang[1], Jeong Ho Kim[1] and Tong Seop Kim[2,*]

[1]*Graduate School, Inha University, Incheon 402-751, Korea*
[2]*Dept. of Mechanical Engineering, Inha University, Incheon 402-751, Korea*

(Manuscript Received November 9, 2012; Revised January 13, 2013; Accepted March 1, 2013)

Abstract

The influence of steam injection and hot gas bypass on the performance and operation of a combined heat and power (CHP) system using a recuperative cycle gas turbine was investigated. A full off-design analysis was used to investigate not only the change in performance but also the variation in engine operation caused by steam injection. The performance improvement capability and operating limitations of full steam injection was examined. Selected operations (partial steam injection and underfiring) that secure minimum compressor surge margin were comparatively analyzed. Partial steam injection was found to be a better option than underfiring in all thermodynamic aspects. Under ISO condition, power and efficiency improvements in the partial injection targeted at a 10% surge margin are 27% and 7.4%, respectively. This study also investigated the increase in steam generation brought by the bypass of turbine exhaust gas around the recuperator. This bypass provided high operational flexibility by varying the capacity of thermal energy supply in both the pure CHP operation and the steam-injected operation. In particular, in the steam-injected operation, the capacity of thermal energy supply can be largely increased by the said bypass, while producing a greater power output than the pure CHP system.

Keywords: Recuperative cycle gas turbine; Full steam injection; Partial steam injection; Underfiring; Surge margin; Hot gas bypass

1. Introduction

Small gas turbines in the power range of hundreds of kilowatts (kW) to several megawatts (MWs) are suitable for combined heat and power (CHP) applications. In such a small power class, power generation efficiencies of simple cycle gas turbines (low 30 s) are not as high as those of large gas turbines for centralized power stations (high 30 s to low 40 s). The simplest solution to enhance the efficiency of small gas turbines is to recover the turbine exhaust heat and preheat the air flowing into the combustor (i.e., to design a recuperative cycle). Micro gas turbines are ideal examples of recuperative cycle gas turbines. Efforts to develop MW-class gas turbines with efficiencies comparable with those of large frame engines have also been made.

In general, seasonal variation in the ratio between heat and power demands of CHP systems is usually large. In gas turbine CHP systems, steam or water injection that modulates heat-to-power ratio is a way to cope with such a variation in the demand pattern. Humidification of gas turbines has been researched widely [1]. Steam injection is the simplest and most cost-effective method among various humidification schemes. The major purposes of injecting steam are to mitigate a reduction of power output in hot seasons [2] and to control the heat-to-power production ratio [3]. Historically, diverse fundamental studies on the characteristics of steam-injected cycles have been performed [4-6]. Studies on steam injection have mostly focused on simple cycle gas turbines. However, with the recent advent of recuperative cycle gas turbines in the market, basic studies have also been initiated regarding performance enhancement by steam or water injection. Several works on the influence of steam injection on the performance of recuperative cycle micro gas turbines using both theoretical [7, 8] and experimental [9] methods have been published. A general parametric study on the recuperative cycle including the effect of injection location has been presented as well [10].

Designing a new steam-injected gas turbine is not economical because such a development entails a full revision of many components. Therefore, injection of steam to an existing engine with minimum hardware modifications is more practical. However, previous studies have mostly offered theoretical results for design mode calculations. Steam injection in an existing engine changes its operating condition, and critical factors, such as compressor surge, may hinder the achieve-

*Corresponding author. Tel.: +82 32 860 7307, Fax.: +82 32 868 1716
E-mail address: kts@inha.ac.kr
† Recommended by Associate Editor Man-Yeong Ha

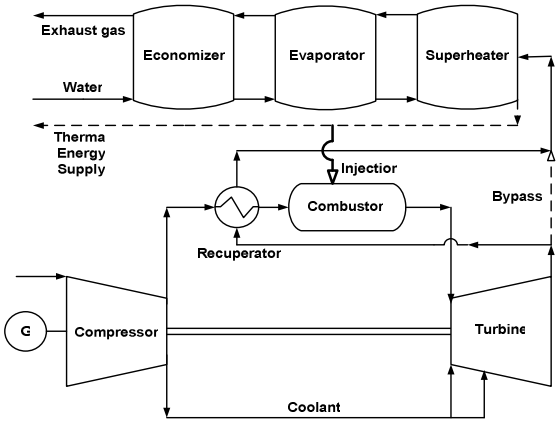

Fig. 1. Schematic diagram of the CHP system using a recuperative cycle gas turbine.

ment of enhanced theoretical performance predicted by design mode calculations. An example of the effect of surge margin control in the simple cycle gas turbine was presented in Ref. [11]. Therefore, an exact off-design analysis that accounts for practical operating issues is important to understand practically achievable performance enhancement. However, only a few off-design (operating mode) analyses have been published. A recent study [8] presented simulation results on the steam and water injection effect in a recuperative cycle micro gas turbine. The major research finding was on the dependence of changes in performance and operating condition on the injection medium (water or steam) and injection location.

In this study, a CHP system using a commercially available 5 MW class of recuperative cycle gas turbine is modeled, and a full off-design analysis is carried out in a wide ambient temperature range to investigate the effect of steam injection. Special attention is given to the change in the compressor surge margin. Operating modes that secure minimum surge margin are simulated, and their influences on engine performance are analyzed. In addition, bypass of turbine exhaust gas around the recuperator is simulated, and its usefulness in controlling heat-to-power ratio is investigated.

2. System and modeling

Fig. 1 shows the schematic layout of the CHP system using a recuperative cycle gas turbine. In the pure CHP mode operation, steam generated at the heat recovery steam generator (HRSG) is used solely for supplying thermal energy to the demand side. In the steam injection operation, the generated steam is injected into the combustor. The design specification of the gas turbine was set up on the basis of a commercially available engine. The net power output and efficiency of the engine are 4.6 MW and 38.5%, respectively [12, 13]. Both the full and partial injections of generated steam were simulated. Moreover, the influence of the bypass of some of the turbine outlet gas on the system performance and operation was examined. Simulations were performed using GateCycle [14].

Table 1. Design parameters and specifications of the gas turbine.

Inlet	Air temperature (K)	288.2
	Air pressure (kPa)	101.3
	Pressure loss (%)	0.5
Compressor	Pressure ratio	9.9
	Number of stages	10
	Isentropic efficiency (%)	86.6
Combustor	Fuel flow rate (kg/s)	0.242
	Fuel lower heating value (kJ/kg)	49,300
	Pressure loss (%)	3.0
Recuperator	Effectiveness (%)	91.0
	Hot side Pressure loss (%)	1.5
	Cold side Pressure loss (%)	1.0
	Energy loss (%)	2.0
Turbine	Turbine inlet temperature (K)	1,466.5
	Exhaust temperature (K)	657.1
	Number of stages	2
	Stage efficiency (%)	80.6
	Total coolant flow relative to compressor inlet air flow (%)	10.0
Exhaust gas	Pressure (kPa)	101.3
	Gas flow rate (kg/s)	17.73
	Pressure loss (%)	0.5
Performance	Gearbox efficiency (%)	98.1
	Generator efficiency (%)	98.1
	Power (kW)	4,600
	Thermal efficiency (%)	38.5

The design point of the gas turbine was simulated on the basis of published design specifications [12, 13] and a previous study [15] where the same engine was simulated. Component design information, such as number of compressor stages, number of turbine stages, and coolant bleed positions, was also adopted from those in literature. Component characteristic parameters, such as the compressor and turbine stage efficiencies, the recuperator effectiveness, and the turbine coolant flow rates, were tuned such that the calculated design specifications, including power, efficiency, exhaust gas flow rate, and turbine inlet and exhaust gas temperatures, coincided with published data. Table 1 lists the major design parameters of the gas turbine. Gas turbine efficiency is defined as follows:

$$\eta_{GT} = \frac{\dot{W}_{GT}}{(\dot{m} \cdot LHV)_{fuel}} . \quad (1)$$

Natural gas served as fuel. Off-design simulation was required to predict the performance variation of the engine caused by ambient temperature change and steam injection. Off-design models of the compressor and the turbine as well as their match are the primary requirements for the simulation of engine operation. As the manufacturer's compressor per-

formance map was not available, several general maps [14] were tried, and the one that made the predicted engine performance closest to the manufacturer's data for a wide ambient temperature range was selected. The compressor map with predicted operating lines is shown in Fig. 6. The surge margin, defined in the following equation, was 20% at the design point.

$$\text{Surge margin} = \frac{PR_{surge} - PR_{operation}}{PR_{operation}} . \quad (2)$$

Turbine operation was modeled by the following choking equation:

$$\frac{\dot{m}_{in}\sqrt{T_{in}}}{\kappa A_{in} P_{in}} = \text{constant, where } \kappa = \sqrt{\frac{\gamma}{R}\left(\frac{2}{\gamma+1}\right)^{\frac{\gamma+1}{\gamma-1}}} . \quad (3)$$

The following equation [16] was adopted to simulate the coolant flow variation caused by the change in operating condition:

$$\dot{m}_{cl} = \dot{m}_{cl,d}\left(\frac{P_{cl}}{P_{cl,d}}\right)\left(\frac{T_{cl,d}}{T_{cl}}\right)^{0.5} . \quad (4)$$

Pressure drops at all flow elements, such as ducts and the recuperator, were corrected using the following equation [17], which considers the changes in flow rate and flow properties:

$$\frac{\Delta P}{\Delta P_d} = \left(\frac{\dot{m}}{\dot{m}_d}\right)^{1.84}\left(\frac{T}{T_d}\right)^{1}\left(\frac{P}{P_d}\right)^{-1} . \quad (5)$$

The heat transfer model of the recuperator, which is a counter-flow primary surface type of heat exchanger, was described by the following equation:

$$NTU \equiv \frac{UA}{\left(\dot{m}c_p\right)_{\min}} = f(\varepsilon) \text{ where, } \varepsilon = \frac{\dot{Q}_{actual}}{\dot{Q}_{\max}} . \quad (6)$$

Once the thermodynamic properties, such as cold and hot stream temperatures at both ends of the recuperator and their flow rates, were obtained from the design calculation, the number of transfer units (NTU) was determined by the NTU-effectiveness relation. Then, the thermal size of the recuperator at the design point, $(UA)_d$, was determined. The hot- and cold-side areas were assumed to be identical, and similar hA values were assigned to both sides at the design point to satisfy the given $(UA)_d$ value according to the following equation:

$$\frac{1}{UA} = \frac{1}{(hA)_h} + \frac{1}{(hA)_c} . \quad (7)$$

Table 2. Design parameters of HRSG.

Inlet water temperature (K)	288.2
Inlet water pressure (kPa)	2,000
Pinch temperature difference (K)	10
Economizer exit sub-cooling (K)	10
Gas-steam approach temperature difference (K)	30
Water & steam pressure drop at each section (%)	3.0
Pressure drop at gas side (%)	3.0
Heat loss at each section (%)	1.0

In off-design operations, the recuperator effectiveness varies with the change in heat transfer characteristics. The major contribution of its variation is due to the change in heat transfer coefficients, which is primarily caused by mass flow change. The following model was used to account for the variation.

$$hA = (hA)_d\left(\frac{\dot{m}}{\dot{m}_d}\right)^{0.3} . \quad (8)$$

The exponent was set at 0.3 with based on Ref. [18]. Separate treatment of hot and cold sides enabled the simulation of bypassing hot gas flow around the recuperator. For the off-design simulation, the same principle described by Eq. (6) was used, but the calculation sequence was reversed. Given the heat transfer coefficients at both the hot and cold sides calculated by Eq. (8), the UA value was calculated by Eq. (7). Then, NTU was calculated using its definition and the UA value in Eq. (6). Finally, the NTU-effectiveness relation produced the off-design effectiveness value.

The HRSG consists of three heat exchanger sections: economizer, evaporator, and superheater. The design parameters of the HRSG shown in Table 2 were determined based on Ref. [4]. The heat transfer performance of each section was corrected in the off-design simulation. The correction procedure of the heat transfer rate of the HRSG is similar to that of the recuperator. The overall heat transfer coefficient was corrected according to the change in the gas-side flow rate [15, 19] as follows:

$$UA = (UA)_d\left(\frac{\dot{m}}{\dot{m}_d}\right)^{0.8} . \quad (9)$$

The HRSG off-design calculation sequence is similar to that of the recuperator calculation: NTU is estimated, effectiveness is calculated according to the NTU-effectiveness relation, and then the heat transfer rate is calculated.

Table 3 summarizes the design performance of the entire CHP system. The power output and efficiency of the gas turbine in the is slightly lower than the nominal values in Table 1

Table 3. Design performance of the CHP system.

Gas turbine power output (kW)	4,501
Gas turbine efficiency (%)	37.94
HRSG inlet gas temperature (K)	658.1
HRSG outlet gas temperature (K)	435.1
Heat recovery (kW)	4,212
CHP efficiency (%)	73.45
Generated steam flow (kg/s)	1.364

Table 4. Summary of various operation modes.

Mode	Description	Steam injection	TIT
CHP	Pure CHP operation	None	Design value
FSI	Full steam injection	Full	Design value
PSI	Partial steam injection to meet 10% surge margin	Partial	Design value
FSI-UF	Full steam injection with underfiring to meet 10% surge margin	Full	decreased

because the CHP system includes an additional pressure drop at the HRSG.

3. Steam injection and hot gas bypass

Table 4 summarizes the four operating modes compared in this study. "CHP" indicates the pure CHP operation where the generated steam at the HRSG is not injected into the gas turbine but entirely used for thermal energy supply. "FSI" denotes full steam injection: steam generated from the HRSG is injected into the gas turbine. In general, the increase in turbine gas flow by steam injection causes the turbine inlet pressure, i.e., the compressor discharge pressure, to rise according to compressor and turbine matching, thereby reducing the surge margin. Therefore, full steam injection may cause an unacceptably low surge margin that cannot be realized in certain conditions [11]. Such critical operations in the current gas turbine will be illustrated in the results. Three approaches to avoid an excessively low surge margin were simulated and compared. A value of 10% was assumed to be a practically acceptable minimum surge margin. "PSI" and "FSI-UF" in Table 5 denote partial steam injection and underfiring, respectively. In PSI, the turbine inlet temperature (TIT) is maintained at the design value, but only a part of the generated steam is injected to maintain the 10% surge margin. In UF, TIT is reduced to meet the same minimum surge margin but all of the generated steam is injected.

Injecting steam into the gas turbine enhances electric power output but reduces the capacity for thermal energy supply. If the thermal energy demand is small compared with the increased electric power demand (i.e., if the site-required heat-to-power ratio is small), the full injection operation could be a viable solution. However, if the thermal energy demand is high, another operating strategy needs to be used. In the recuperative cycle, the heat recovery rate at the HRSG depends on the heat transfer rate at the recuperator, which is located prior to the HRSG. Therefore, if the heat transfer rate of the recuperator could be varied, the HRSG heat recovery (i.e., steam generation) could be modulated to some extent. For this reason, the effect of bypassing some of the hot gas from the turbine to the downstream of the recuperator was analyzed (see Fig. 1). The bypass would benefit both normal CHP operation and steam injection operation because the capacity of thermal energy supply can be increased by the bypass while electric power is kept at the level of demand. As the fraction of bypassed hot gas increases, the HRSG inlet gas temperature rises, which in turn generates more steam. Then, for a required electric power augmentation, which can be achieved by injecting a certain amount of steam, the available steam for thermal energy supply increases.

4. Results and discussion

4.1 Pure CHP operation

The result for pure CHP operation without steam injection and hot gas bypass is examined as a reference case. Power output, power generation efficiency, and available thermal energy produced at the HRSG are shown as functions of ambient temperature in Fig. 2. TIT is maintained at the design value in all conditions in the figure, i.e., full-load operating performance at all ambient conditions. Variations in the ratio between the generated steam and the gas turbine inlet air flow as well as those in the surge margin are shown in Fig. 3. Power and the efficiency decreased with increasing ambient temperature, following the natural trend. Power variation data from the brochure of the manufacturer of the gas turbine are also drawn. The slight discrepancy between the simulation data and the brochure data is due to the fact that simulated power output was calculated for the CHP system where pressure loss in the HRSG was included, whereas the manufacturer's data were given for simple gas turbine operation without additional pressure loss (refer to the last paragraph of section 2). The study confirmed in a separate calculation that the simulation would produce almost the same power output as the reference data without pressure loss in the HRSG. The close agreement indicated the feasibility of the adopted compressor performance map and other off-design models. Heat recovery is insensitive to ambient temperature. Exhaust flow in the gas turbine decreased as the ambient temperature increased. However, the gas turbine exhaust temperature, i.e., HRSG inlet gas temperature, increased with increasing ambient temperature. These two counteracting factors resulted in the relatively flat variation (a slight maximum at around 10°C) in the recovered thermal energy.

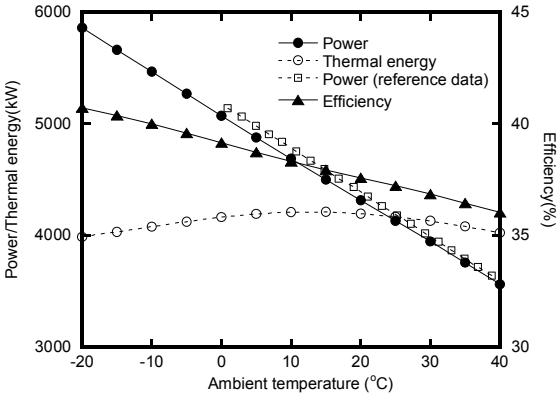

Fig. 2. Performance variation of the pure CHP operation with ambient temperature.

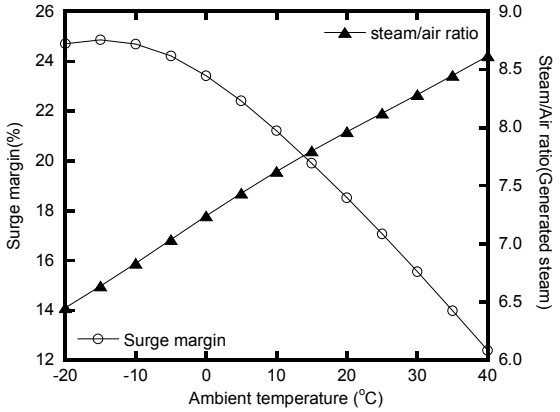

Fig. 3. Variations in the compressor surge margin and the steam/air ratio of the pure CHP operation with ambient temperature.

The surge margin decreased as the ambient temperature became higher. However, it remained greater than 10% even at 40°C of ambient condition, which indicates that stable operation is possible up to a very high temperature. The steam flow amounted to 7.8% of the inlet air flow at 15°C of ambient temperature. The steam/air ratio increased as the ambient temperature rose because a higher ambient temperature would lead to a higher HRSG inlet gas temperature.

4.2 Steam-injected operation

Figs. 4 and 5 show the surge margin and the ratio between the injected steam flow and the gas turbine inlet air flow in three steam-injected operations. In FSI, steam production, which is the same as the injected steam, was greater than that in the pure CHP operation. This finding was attributed to increases in both the mass flow and the specific heat of the hot gas stream at the HRSG compared with the pure CHP operation. Injecting such a large amount of steam into the gas turbine raised the compressor discharge pressure, resulting in a drastic reduction of the surge margin. In almost all ambient conditions, the surge margin of fully injected operations fell

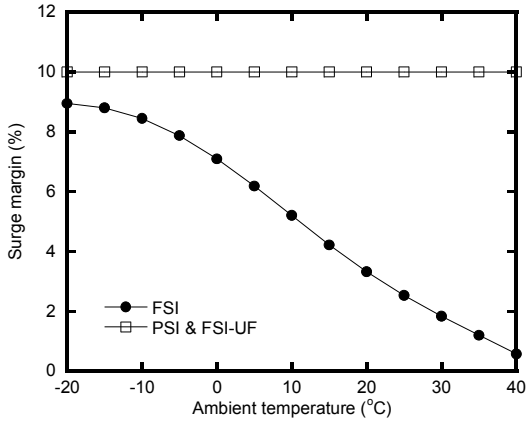

Fig. 4. Variations in the compressor surge margin of the steam-injected operations with ambient temperature.

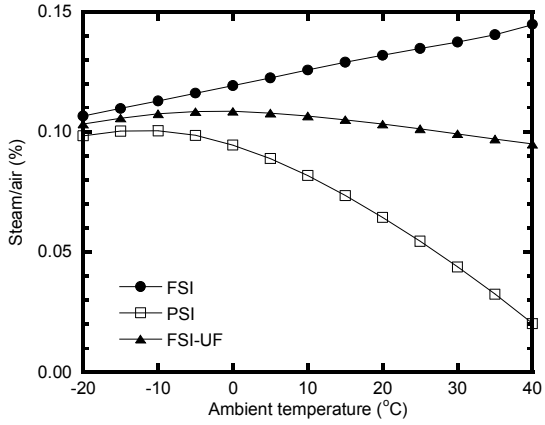

Fig. 5. Variations in the injected steam/air ratio of the steam-injected operations with ambient temperature.

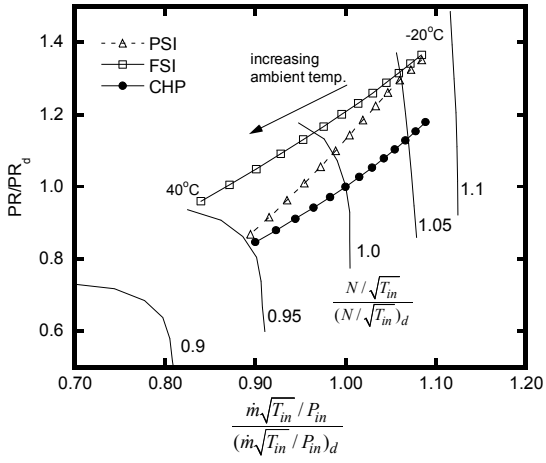

Fig. 6. Running lines of different operations on the compressor map.

below 10%. In particular, it approached zero as the temperature rose over typical summer conditions. Fig. 6 shows the compressor running lines of different operating modes, which clearly shows that steam injection pushes the operating point

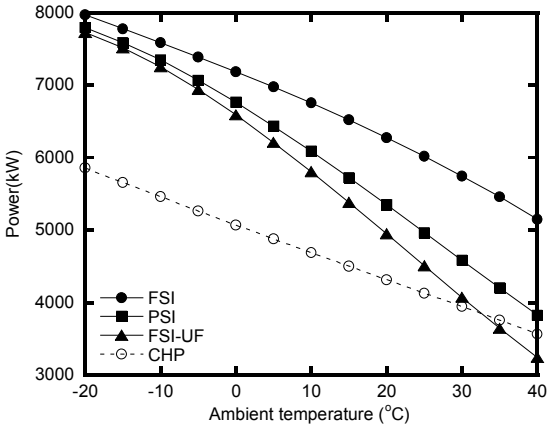

Fig. 7. Variation in the power output of the steam-injected operations with ambient temperature.

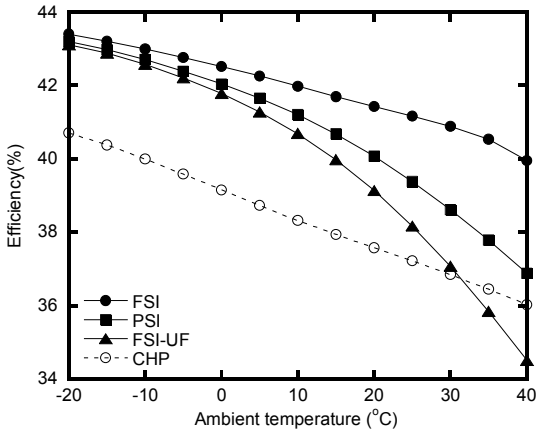

Fig. 8. Variation in the power generation efficiency variation of the steam-injected operations with ambient temperature.

toward the surge point.

Such a small surge margin is not allowable from the view point of engine safety. The allowable minimum surge margin may depend on various factors, which are suggested by engine manufacturers. In this work, a case study was undertaken to present the effect of surge margin control, with 10% surge margin as a guideline. As described in Table 4, two methods were introduced to restore the surge margin to 10%: FSI-UF and PSI (see the constant or flat surge margin in the two operations in Fig. 4). In both FSI-UF and PSI, the amount of injected steam decreased compared with that in FSI. In case of PSI, the total steam production at the HRSG was larger than the injected amount shown in Fig. 5. To satisfy the minimum surge margin, the injected steam was decreased as the ambient temperature rose. This step was taken because the surge margin of the pure CHP operation was already sufficiently low (slightly higher than 10%) in high-temperature conditions. As shown in Fig. 5, almost the entirety of generated steam can be injected in low ambient condition, but only a very small amount of steam can be injected in the high-temperature region. The operating line of PSI in Fig. 6 shows this trend.

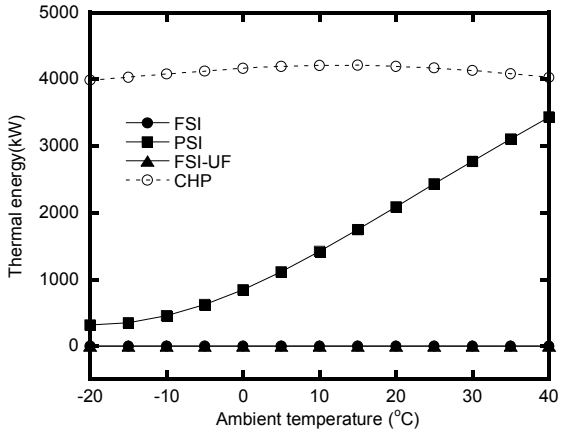

Fig. 9. Variation in the thermal energy of the steam-injected operations with ambient temperature.

The power output and efficiency of the gas turbine in the three steam-injected operations are shown in Figs. 7 and 8, respectively. Those of pure CHP operations were also shown for comparison. As expected, FSI appeared to enhance both power and efficiency considerably compared with the pure CHP operation. The power and efficiency upgrades at 15 °C of ambient temperature were 45% (6,524 kW vs. 4,501 kW) and 10% (3.8% points, 41.7% vs. 37.9%), respectively. Both UF and PSI reduced power and efficiency in comparison with FSI. PSI provided a relatively larger power output and higher efficiency compared with UF. For PSI, power and efficiency improved by 27% and 7.4%, respectively, at 15°C of ambient temperature in comparison with the pure CHP operation. For UF, the performance penalty increased dramatically as the ambient temperature rose. In particular, UF exhibited lower power output and efficiency compared with pure CHP operation in the high-temperature range (over 30°C), which indicated that the TIT reduction caused excessive penalty. In UF operation, the TIT had to be decreased by about 250 K from the design value at 40°C of ambient temperature to meet the 10% surge margin. Fig. 9 shows the variation in the capacity of thermal energy supply, i.e., the energy of the steam not injected. Evidently, no thermal energy is available in the case of FSI and FSI-UF. On the contrary, PSI could provide thermal energy that increases as the ambient temperature rises because of the reduction in the portion of injected steam out of the generated steam.

In conclusion, we obtained the following summary for steam-injected operation. Full injection is superior to any other operations simply in the view point of performance enhancement. However, the compressor surge margin becomes almost zero at very high ambient temperatures under FSI operation. Both PSI and FSI-UF can solve the problem of surge margin reduction, but the former is a better option in all thermodynamic aspects: gas turbine power, efficiency, and availability of thermal energy supply. However, even in PSI, the enhancement of gas turbine performance appears to be marginal

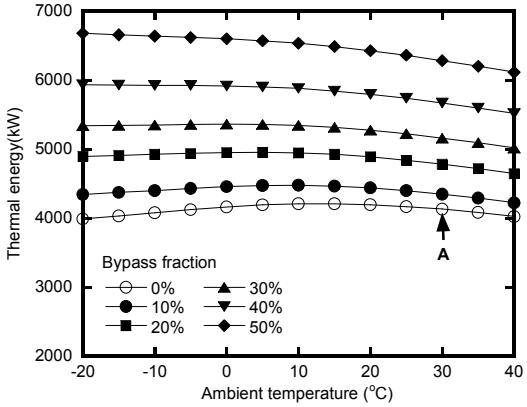

Fig. 10. Effect of the hot gas bypass on the thermal energy of the pure CHP operation.

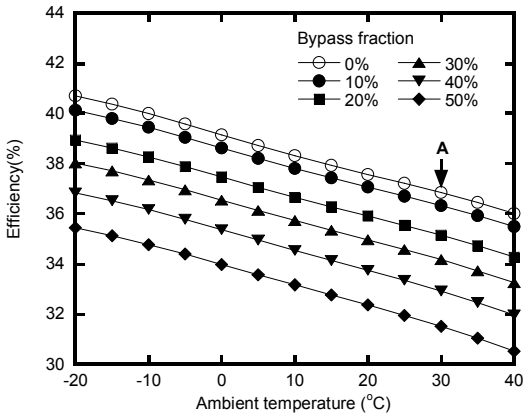

Fig. 11. Effect of the hot gas bypass on the power generation efficiency of the pure CHP operation.

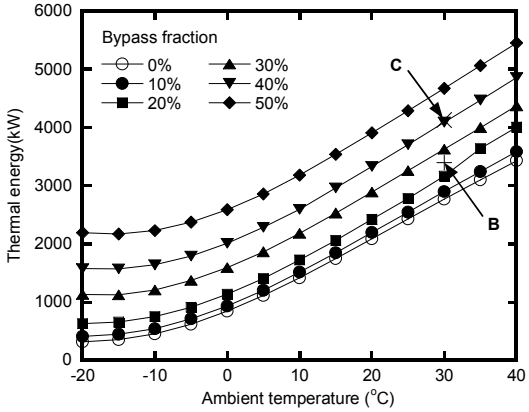

Fig. 12. Effect of the hot gas bypass on the thermal energy of the PSI operation.

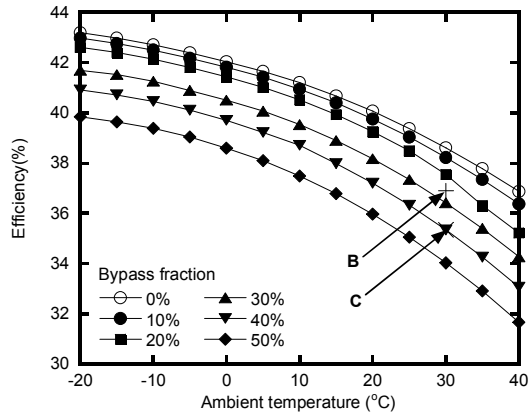

Fig. 13. Effect of the hot gas bypass on the power generation efficiency of the PSI operation.

in the high ambient temperature range because of the limitation in the injected amount. Moreover, a relaxation (reduction) of the minimum surge margin would increase the benefit of steam injection. For example, an extra simulation for the operation at 5% surge margin showed that the relative power augmentation with PSI at 40°C of ambient temperature would increase from 7.4% in the case of 10% surge margin to 24.6% in the case of 5% surge margin. The efficiency enhancement also improved from 0.9% points to 2.5% points.

4.3 Hot gas bypass

The effect of hot gas bypass on system performance was investigated for the pure CHP operation first and then for the PSI operation. When some of the hot gas from the turbine exit was bypassed around the recuperator and mixed with the recuperator exit gas, the steam generation rate increased because the HRSG inlet gas temperature increased. However, the combustor fuel supply increased (i.e., efficiency decreased) because the temperature rise of the cold side air also decreased.

Results for the pure CHP operation are shown in Figs. 10 and 11. The bypass fraction is defined as follows:

$$\text{Bypass fraction} = \frac{\text{bypassed flow}}{\text{total turbine exit flow}}. \quad (10)$$

The bypass increased the thermal energy (i.e., the generated steam) recovered at the HRSG as expected. More than 50% increase was expected from bypassing half of the hot gas. However, the increase in the bypass fraction inevitably caused a loss in power generation efficiency. The efficiency penalty with 50% bypass was more than 5% points. The gas turbine power output slightly increased with increasing bypass fraction because of a reduction in the pressure loss at the hot side of the recuperator. However, as the effect was marginal, the power output remained effectively constant (i.e., similar to the power output depicted in Fig. 2). In summary, the hot gas bypass can help manage the varying heat-to-power demand ratio, but the efficiency penalty is a disadvantage.

The effect of hot gas bypass on steam-injected operation is illustrated for PSI with 10% surge margin. The influences of hot gas bypass on power output, thermal energy, and efficiency are presented in Figs. 12 and 13. Gas turbine power output was very insensitive to the hot gas bypass as in the pure CHP case (i.e., similar to the power output depicted in Fig. 7).

The bypass considerably enhanced the capacity of thermal energy supply as in the pure CHP operation. The power generation efficiency decreased with increasing bypass fraction, but the degree of efficiency penalty was less than that in the pure CHP operation (compare results of Figs. 11 and 13). In summary, the capacity of thermal energy supply can be modulated by controlling the hot gas bypass, while maintaining the same level of power augmentation. Therefore, a flexible operation depending on the heat-to-power demand ratio, especially on the variation in thermal energy demand, is possible.

Operational flexibility provided by the gas bypass can be illustrated as follows. The pure CHP operation at 30°C (i.e., the point A in Figs. 10 and 11) exhibits 3,940 kW electric power, 36.9% power generation efficiency, and 4,130 kW thermal energy. With PSI operation at the same ambient temperature, the power generation efficiency would be higher than that of the pure CHP operation (36.9%) at up to 25% of hot gas bypass (point B). At point B, the thermal energy would be less than that of the pure CHP operation (3,400 kW vs. 4,130 kW) but considerably greater than that of the PSI operation without bypass (2,770 kW). Evidently, the electric power output would be much greater than that of the pure CHP operation (4,580 kW vs. 3,940 kW). If thermal energy demand becomes even greater, some more gas can be bypassed, while maintaining the electric power output. For example, point C (40% of bypass) exhibits the same thermal energy as the pure CHP operation. Under this condition, the power generation efficiency becomes lower than that of the pure CHP operation (35.4% vs. 36.9%). This example demonstrates that hot gas bypass compensates for the shortcoming of the steam-injected operation, i.e., reduced thermal energy supply, while maintaining its advantage, i.e., greater power. Thus, the thermal energy can be greatly increased (can be even larger than under the pure CHP operation), and power generation efficiency can be higher than that of the pure CHP operation for a wide bypass fraction range.

5. Conclusion

The results of this study are summarized as follows.

(1) Steam injection enhances both power and efficiency of the regenerative cycle gas turbine considerably. By injecting the full amount of the generated steam, the power and efficiency could be improved by 45% and 10%, respectively, under ISO condition. However, FSI is accompanied by a considerable reduction in the compressor surge margin because of the increased mass flow rate of the turbine, leading to unacceptably small surge margins in high ambient temperatures.

(2) To avoid excessive surge margin reduction, two strategies were investigated: PSI and UF. Both operations were intended to maintain the 10% surge margin under any operating condition. PSI was found to be a better option in all thermodynamic aspects: power output, efficiency, and available thermal energy supply. The power and efficiency improvement with PSI under ISO condition was 27% and 7.4%, respectively. The advantage diminishes as the ambient temperature increases.

(3) The influence of the bypass of some of the turbine exhaust gas flow around the recuperator on the operation and performance characteristics was also investigated. The bypass provides high operational flexibility by varying the capacity of thermal energy supply in both pure CHP operation and steam-injected operation. In particular, in the steam-injected operation, the capacity of thermal energy supply can be largely increased by the bypass, while producing greater power output than the pure CHP system. A considerably large bypass allows the steam-injected operation to exhibit a larger thermal energy supply as well as a larger electric power output than the pure CHP operation. Moreover, the power generation efficiency is higher than that of the pure CHP operation in a wide bypass fraction range.

Acknowledgment

This work was supported by the Inha University Research Grant.

Nomenclature

A : Area [m^2]
c_p : Constant pressure specific heat [kJ/kg·K]
CHP : Combined heat and power
FSI : Full steam injection with full firing
FSI-UF: Full steam injection with underfiring
GT : Gas turbine
HRSG : Heat recovery steam generator
h : Heat transfer coefficient [kW/m^2K]
LHV : Lower heating value [kJ/kg]
$\dot{m}$: Mass flow rate [kg/s]
NTU : Number of transfer units
P : Pressure [kPa]
ΔP : Pressure loss [kPa]
PSI : Partial steam injection
PR : Pressure ratio
$\dot{Q}$: Heat transfer rate [kW]
R : Gas constant [kJ/kg·K]
T : Temperature [K]
TIT : Turbine inlet temperature [K]
U : Overall heat transfer coefficient [kW/m^2K]
$\dot{W}$: Power [kW]
ε : Heat exchanger effectiveness
γ : Specific heat ratio
η : Efficiency
κ : Constant

Subscripts

c : Cold side

cl : Coolant
d : Design
h : Hot side
in : Inlet

References

[1] M. Jonsson and J. Yan, Humidified gas turbines-a review of proposed and implemented cycles, *Energy*, 30 (2005) 1013-1078.

[2] A. Bouam, S. Aissani and R. Kadi, Combustion chamber steam injection for gas turbine performance improvement during high ambient temperature operations, *Trans. ASME J. of Engineering for Gas Turbines and Power*, 130 (2008) 1-10.

[3] D. Y. Cheng and L. C. Nelson, The chronological development of the Cheng cycle steam injected gas turbine during the past 25 years, *ASME paper* GT2002-30119 (2002).

[4] O. Bolland and F. J. Stadaas, Comparative evaluation of combined cycles and gas turbine systems with water injection, steam injection, and recuperation, *Trans. ASME J. of Engineering for Gas Turbines and Power*, 117 (1995) 138-145.

[5] M. De Paepe and E. Dick, Cycle improvements to steam injected gas turbines, *Int. J. Energy Res*, 24 (2000) 1081-1107.

[6] R. Yadav and P. Kumar, Comparative thermodynamic analysis of combined and steam injected gas turbine cycles, *ASME paper* IJPGC2003-40118 (2003).

[7] F. Delattin, S. Bram, S. Knoops and D. J. Ruyck, Effects of steam injection on microturbine efficiency and performance, *Energy*, 33 (2008) 241-247.

[8] J. J. Lee, M. S. Jeon and T. S. Kim, The influence of water and steam injection on the performance of a recuperated cycle microturbine for combined heat and power application, *Applied energy*, 87 (2010) 1307-1316.

[9] T. Tsuchiya, M. Okamoto, S. Shibata and K. Mochizuki, Improvement of micro gas turbine performance by steam injection, *Proceedings of the Asian Congress on Gas Turbines*, ACGT 2005-068 (2005).

[10] K. Nishida, T. Takagi and S. Kinoshita, Performance analysis of regenerative steam injection gas turbine (RSTIG) systems, *ASME paper*, GT2003-38823 (2003).

[11] S. Y. Kang and T. S. Kim, Changes in performance and operating condition of a gas Turbine combined heat and power system by steam injection - a focus on compressor operation, *Journal of Fluid Machinery*, 14 (2012) 68-75. (in Korean).

[12] http://mysolar.cat.com/cda/files/126873/7/dsm50pg.pdf.

[13] W. L. Lundberg, S. E. Veyo and M. D. Moeckel, A high-efficiency solid oxide fuel cell hybrid power system using the mercury 50 advanced turbine systems gas turbine, *Trans. ASME J. of Engineering for Gas Turbines and Power*, 125 (2003) 51-58.

[14] GE Enter Software, 2006, GateCycle, ver. 6.0.

[15] D. W. Kang, T. S. Kim, K. B. Hur and J. K. Park, The effect of firing biogas on the performance and operating characteristics of simple and recuperative cycle gas turbine combined heat and power systems, *Applied Energy*, 93 (2012) 215-228.

[16] C. A. Palmer, M. R. Erbes and P. A. Pechtl, GateCycle performance analysis of the LM2500 gas turbines utilizing low heating value fuels, *ASME Cogen Turbo Power '93*, 8 (1993) 69-76.

[17] M. R. Erbes and R. R. Gay, Gate/Cycle predictions of the off-design performance of combined-cycle power plants, Simulation of Energy Systems, *ASME HTD*, 124 (1989) 43-51.

[18] T. S. Kim and S. H. Hwang, Part load performance analysis of recuperated gas turbines considering engine configuration and operation strategy, *Energy*, 31 (2006) 260-277.

[19] R. Kehlhofer, Calculation for part-load operation of combined gas/steam turbine plants, *Brown Boveri Rev*, 65 (1978) 672-679.

S. Y. Kang received his M.S. degree from the Department of Mechanical Engineering, Inha University, in 2010 and is presently a doctoral student in the same department. His major research topic is performance analysis of energy and power generation systems.

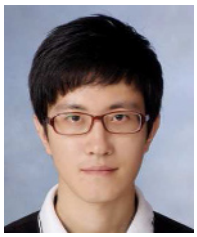

J. H. Kim received his B.S. degree from the Department of Mechanical Engineering, Inha University, in 2011 and is currently a master's degree student in the same department. His major research topic is the simulation of gas turbine operation.

T. S. Kim received his Ph.D. degree from the Department of Mechanical Engineering, Seoul National University, in 1995. He has been with the Dept. of Mechanical Engineering, Inha University, since 2000. His research interests are the design and analysis of advanced energy systems, including gas/steam turbine-based power plants.